

## Relaxation Dynamics, Softness, and Fragility of Microgels with Interpenetrated Polymer Networks

Valentina Nigro, Barbara Ruzicka, Beatrice Ruta, Federico Zontone, Monica Bertoldo, Elena Buratti, Roberta Angelini

► **To cite this version:**

Valentina Nigro, Barbara Ruzicka, Beatrice Ruta, Federico Zontone, Monica Bertoldo, et al.. Relaxation Dynamics, Softness, and Fragility of Microgels with Interpenetrated Polymer Networks. *Macromolecules*, American Chemical Society, 2020, 53 (5), pp.1596-1603. 10.1021/acs.macromol.9b01560. hal-02524013

**HAL Id: hal-02524013**

**<https://hal.archives-ouvertes.fr/hal-02524013>**

Submitted on 26 Nov 2020

**HAL** is a multi-disciplinary open access archive for the deposit and dissemination of scientific research documents, whether they are published or not. The documents may come from teaching and research institutions in France or abroad, or from public or private research centers.

L'archive ouverte pluridisciplinaire **HAL**, est destinée au dépôt et à la diffusion de documents scientifiques de niveau recherche, publiés ou non, émanant des établissements d'enseignement et de recherche français ou étrangers, des laboratoires publics ou privés.

# Relaxation dynamics, Softness and Fragility of Microgels with Interpenetrated Polymer Networks

Valentina Nigro,<sup>1,2,\*</sup> Barbara Ruzicka,<sup>1,2,\*</sup>  
Beatrice Ruta,<sup>3,4</sup> Federico Zontone,<sup>4</sup> Monica Bertoldo,<sup>5</sup>  
Elena Buratti,<sup>1</sup> and Roberta Angelini<sup>1,2,\*</sup>

<sup>1</sup> Istituto dei Sistemi Complessi del Consiglio Nazionale delle Ricerche (ISC-CNR),  
sede Sapienza, Pz.le Aldo Moro 5, I-00185 Roma, Italy

<sup>2</sup> Dipartimento di Fisica, Sapienza Università di Roma, I-00185, Italy

<sup>3</sup> France Univ Lyon, Université Claude Bernard Lyon 1, CNRS, Institut Lumière Matière, Villeurbanne, France

<sup>4</sup> ESRF The European Synchrotron, CS40220, 38043 Grenoble Cedex 9, France

<sup>5</sup> Istituto per la Sintesi Organica e la Fotoreattività  
del Consiglio Nazionale delle Ricerche (ISOF-CNR), via P. Gobetti 101, 40129 Bologna, Italy

\*To whom correspondence should be addressed;

E-mail: valentina.nigro@uniroma1.it (V.N), barbara.ruzicka@roma1.infn.it (B.R.),  
roberta.angelini@roma1.infn.it (R.A.).

**Microgels are elastic and deformable particles with a hybrid nature between that of polymers and colloids and unconventional behaviours with respect to hard colloids. We investigated the dynamics of a soft microgel made of interpenetrated polymer networks of PNIPAM and PAAc by means of coherent X-ray and light scattering techniques. By varying the particle softness through PAAc content we can tune at wish the fragility of IPN microgels. Interestingly we find the occurrence of a dynamical crossover at a critical packing fraction which leads to an evolution of the structural relaxation time from super-Arrhenius to Ar-**

rhenius, a minimum for the shape of the intensity autocorrelation function and the emerging of distinct anomalous mechanisms for particle motion. This complex phenomenology can be modelled by a Fickian diffusion at very low concentrations, an effective non Fickian anomalous diffusion at intermediate values and a ballistic motion well described within the Mode Coupling Theory on approaching the glassy state.

## 1 Introduction

In the last decades many works have been focused on the study of the glass transition in complex systems aiming at understanding differences and similarities between structural glasses (SG) and colloidal glasses (CG) (1, 2). In the case of structural glasses, as the liquid is rapidly quenched below its melting temperature, it undergoes a glass transition avoiding nucleation and crystallization. In colloids the transition is instead triggered by volume fraction  $\phi$  or waiting time  $t_w$  (signaled by an aging phenomenon) whose increase drives the systems in an out-of-equilibrium configuration. Changing control parameters like temperature, packing fraction or aging time, the dynamics of both structural and colloidal glasses slows down enormously and is accompanied by a dramatic increase of the characteristic relaxation time ( $\tau(T)$ ,  $\tau(\phi)$ ,  $\tau(t_w)$ ) by several orders of magnitude up to the glassy state. The most direct way to access microscopic information on the relaxation dynamics is to look at the evolution of the intensity autocorrelation functions which are well described by the Kohlrausch-Williams-Watts (KWW) expression  $F(Q, t) \propto \exp(-(t/\tau(Q))^\beta)$  where  $\tau$  is an "effective" relaxation time and  $\beta$  measures the distribution of relaxation times and assumes generally positive values  $\beta < 1$  (stretched behaviour). Recently an anomalous dynamics, characterized by a shape parameter  $\beta > 1$  (compressed behaviour), has emerged in out of equilibrium states of different materials like colloidal glasses (3–10), gels (11–13), supercooled liq-

uids (14, 15), metallic glasses (16, 17), polymeric systems (18–20), ceramics (21) and investigated also in theoretical (22, 23) and simulation (24–27) works. The existence of stretched and/or compressed correlation functions is currently a very debated issue also faced in this work. Despite of many studies on the glass transition in SG and CG several questions are still open: Is the structural relaxation behaviour peculiar of the specific investigated system? How does it depend on the control parameters? What is the  $\beta$  parameter behaviour? What happens to the diffusive dynamics of the equilibrium liquid? Combining X-ray Photon Correlation Spectroscopy (XPCS) and Dynamic Light Scattering (DLS), we answer these questions investigating the behaviour of the structural relaxation time and  $\beta$  exponent for a soft colloid. Soft colloids are an interesting class of glass-formers that, at variance with hard sphere-like colloids, provide a good tunability of particle softness giving rise to unconventional phase-behaviours (28, 29). They are indeed aqueous suspensions of nanometre- or micrometre-sized hydrogel particles sensitive to external stimuli whose dimension and effective volume fraction can be varied by changing external parameters such as temperature and/or pH.

The most studied responsive microgels are those based on the thermo-sensitive poly(N-isopropylacrylamide) (PNIPAM), with a reversible Volume Phase Transition (VPT) around 305 K. These systems have been largely investigated both theoretically and experimentally (30–36). In this work we study a PNIPAM-based microgel with a second interpenetrated polymer network (IPN) of poly(acrylic acid) (PAAc) (37–42) that provides additional pH sensitivity, topological constraints to the particles and extra charges to the system. In this way the IPN microgel softness can be controlled by synthesis varying the amount of poly(acrylic acid).

## 2 Experimental Methods

The dynamic structure factor has been investigated at different scattering vectors  $Q$ , weight concentrations  $C_w$  and PAAc content  $C_{PAAc}$  through combined XPCS and DLS techniques.

XPCS measurements were performed at ID10 beamline of ESRF in Grenoble using a partially coherent X-ray beam with a photon energy of 21 keV. A series of scattering images were recorded by CdTe Maxipix detector (photon counting). The ensemble averaged intensity autocorrelation function  $g_2(Q, t) = \frac{\langle\langle I(Q, t_0)I(Q, t_0+t) \rangle\rangle_p}{\langle\langle I(Q, t_0) \rangle\rangle_p^2}$ , where  $\langle \dots \rangle_p$  is the ensemble average over the detector pixels mapping onto a single  $Q$  value and  $\langle \dots \rangle$  is the temporal average over  $t_0$ , was calculated by using a standard multiple  $\tau$  algorithm (43). XPCS data were complemented by DLS measurements performed at the CNR-ISC laboratory. The monochromatic and polarized beam emitted from a solid state laser (100 mW at  $\lambda = 642$  nm) was focused on the sample placed in a cylindrical VAT for index matching and temperature control. The scattered intensity was simultaneously collected by single mode optical fibers at five different scattering angles, namely  $\theta=30^\circ, 50^\circ, 70^\circ, 90^\circ, 110^\circ$ , corresponding to different scattering vectors  $Q$ , according to the relation  $Q=(4\pi n/\lambda) \sin(\theta/2)$ .

The investigated samples were IPN microgels synthesized by a sequential free radical polymerization method, then purified, lyophilized and diluted in water to the desired concentration under magnetic stirring for 1 day. A more detailed description of the preparation protocol is reported in Ref. (44, 45). Samples at different concentrations were obtained by dilution at pH close to 5.5. Measurements were performed on aqueous suspensions of IPN microgels at five PAAc content ( $C_{PAAc}=2.6$  %,  $C_{PAAc}=10.6$  %,  $C_{PAAc}=15.7$  %,  $C_{PAAc}=19.2$  %,  $C_{PAAc}=24.6$  %), fixed temperature above the VPTT ( $T=311$  K), different weight concentrations  $C_w=(0.05 \div 5)$  % and acidic pH (pH  $\sim 5.5$ )

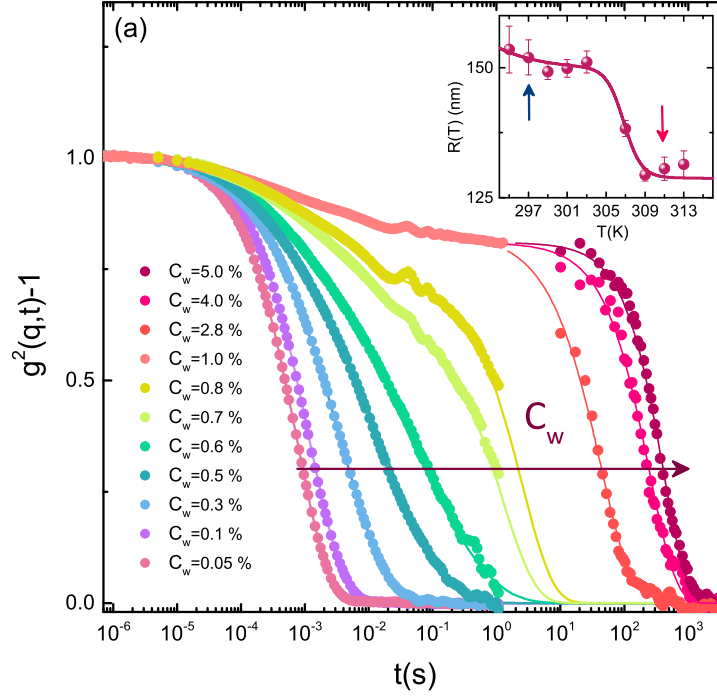


Figure 1: (a) Normalized intensity autocorrelation functions of IPN microgel particles at  $C_{PAAc} = 24.6$  %,  $T = 311$  K and  $Q = 0.022$  nm $^{-1}$  as a function of concentration and (b) Temperature behaviour of the hydrodynamic radius at  $C_w = 0.01$  %, blue and red arrows indicate  $T = 297$  K and  $T = 311$  K respectively.

in the  $Q$  range  $Q = (0.006 \div 0.063)$  nm $^{-1}$  below the peak of the static structure factor. The particles radii of the investigated samples at  $T = 311$  K are:  $C_{PAAc} = 2.6$  %  $R = (26 \pm 1)$  nm,  $C_{PAAc} = 10.6$  %  $R = (52 \pm 2)$  nm,  $C_{PAAc} = 15.7$  %  $R = (68 \pm 3)$  nm,  $C_{PAAc} = 19.2$  %  $R = (89 \pm 2)$  nm,  $C_{PAAc} = 24.6$  %  $R = (130 \pm 2)$  nm; they increase with PAAc content as reported in Ref. (46). An example of the temperature behaviour of hydrodynamic radius for  $C_{PAAc} = 24.6$  % and  $C_w = 0.01$  % is reported in Fig. 1(b).

### 3 Results and Discussion

Figure 1 shows DLS and XPCS intensity autocorrelation functions for IPN microgels with fixed PAAc content ( $C_{PAAc} = 24.6$  %) at different concentrations  $C_w$  and fixed tempera-

ture  $T=311$  K (red arrow in Fig. 1(b)) when the particles are in the shrunken state. At low  $C_w$  the intensity scattering functions are well described by a monomodal decay capturing the particle diffusion in the high dilution limit. As the particle concentration increases a dynamical decoupling is observed and a two-step relaxation, characteristic of glass-forming systems approaching the glass transition, comes out. The monomodal decay for  $C_w < 0.6$  % and the final decay for  $C_w \geq 0.6$  % are well described by the Kohlrausch-Williams-Watts expression (47):

$$g_2(Q,t) = b[(A \exp(-(t/\tau(Q))^\beta))^2 + 1] \quad (1)$$

where  $b \cdot A^2$  is the coherence factor,  $\tau$  the structural relaxation time and  $\beta$  the shape exponent, representing a phenomenological hallmark of glass forming liquid dynamics. The fits are shown as full lines in Fig. 1.

The normalised structural relaxation time is reported in Fig.2(a) as a function of weight concentration  $C_w$  and for different PAAc content  $C_{PAAc}$ . Two main features stand out: firstly the normalised structural relaxation time has a smoother and smoother concentration dependence with decreasing PAAc content and secondly a divergence occurs at lower concentrations for particles with higher PAAc content. This can be related to the increased interactions due to COOH groups belonging to PAAc chains as deeply discussed in Ref. (46). Our data are well described by the super-Arrhenius expression:

$$\tau = \tau_0 \exp\left(\frac{D_{C_w} C_w}{C_{w0} - C_w}\right) \quad (2)$$

where  $C_{w0}$  sets the apparent divergence,  $D_{C_w}$  controls the growth of the structural relaxation time and  $\tau_0$  is the characteristic structural relaxation time in the high dilution limit. This result points out that, by changing PAAc content, different dynamical

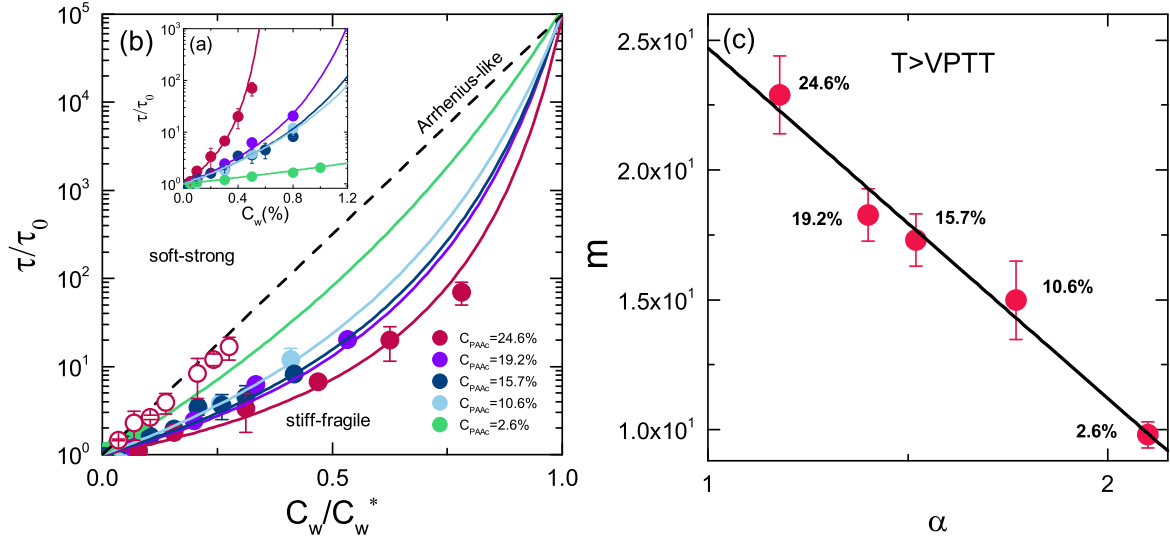


Figure 2: (a) Normalised structural relaxation time as a function of weight concentration at the indicated PAAc contents and  $T=311$  K. Solid lines are fits through Eq.(2). (b) Angell plot for the normalized structural relaxation time versus normalized weight concentration at  $T=311$  K (closed symbols) compared with data at  $T=297$  K for a sample at 24.6 % of PAAc as an example (open symbols). Solid lines are fits according to Eq.(2). (c) Fragility index  $m$  as a function of swelling ratio related to particles softness.

behaviours can be achieved in microgels as in the case of molecular glass formers (48). This is highlighted in Fig.2(b) where the data for each PAAc content are rescaled by a  $C_w$  value, called  $C_w^*$ , at which the relaxation time is the same. At increasing PAAc content the curves depart more and more from the Arrhenius-like behaviour that is recovered only in the case of microgels in the completely swollen state at  $T=297$  K (blue arrow in Fig.1(b)), as shown for the sample at 24.6 % of PAAc (open symbols).

Recently, the unifying concept of fragility has been extended to colloidal suspensions (33, 34, 38, 49, 50) and many efforts have been devoted to understand the effect of softness on fragility (38, 49–52). In this context the slope of the data at  $C_w = C_w^*$  can be used to define a kinetic fragility as:



$$m = \left[ \frac{\partial \log \tau}{\partial (C_w/C_w^*)} \right]_{C_w=C_w^*} \quad (3)$$

Since the pioneering study of Ref. (38) the connection between softness and fragility in soft colloids is still largely debated. A recent work on PNIPAM microgels (Ref. (36)) states that regardless of their softness, soft colloids exhibit the same fragile-like behaviour of hard colloids. Moreover a simple theoretical model (Ref. (49)) has found that depending on osmotic pressure, presence of ions, dimension of particles, osmotic deswelling may be significant, giving rise to strong rather than fragile glasses. Here we show that the fragility can be also finely controlled by tuning the amount of PAAc interpenetrated within PNIPAM network.

To this aim we define the swelling ratio as:

$$\alpha = \frac{R_H^{swollen}}{R_H^{shrunk}} \quad (4)$$

where  $R_H^{swollen} = R(T=297 \text{ K})$  and  $R_H^{shrunk} = R(T=311 \text{ K})$  (blue and red arrows in Fig.1(b) respectively). Particles with higher softness can shrink more, providing a larger value of  $\alpha$  that decreases with increasing PAAc content as reported in Ref. (46). Plotting the fragility  $m$  as a function of  $\alpha$  (Fig.2(c)) we find a linear decrease with increasing particle softness in surprisingly agreement with very recent theoretical results on the role of deformation in soft colloids (50). A clear picture of the relation between softness and fragility is thus provided: the higher is the PAAc content, the stiffer are the particles, yielding thus to more fragile systems. These results compared to previous works (36, 38, 49) corroborate the idea that soft colloids can give rise to both fragile and strong behaviours. In our system the interpenetration of PAAc determines an increase of topological constraints, an increase of particle dimensions and extra charges.

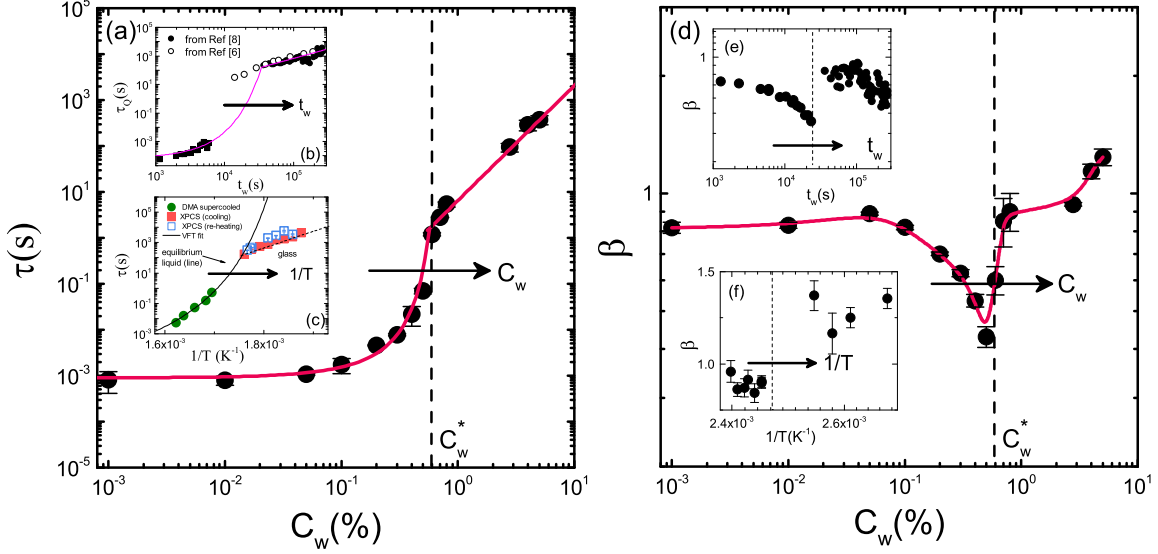


Figure 3: (a) Structural relaxation time from Eq.(1) as a function of weight concentration for IPN microgel suspensions at  $C_{PAAc}=24.6\%$ ,  $T=311\text{ K}$  and  $Q=0.022\text{ nm}^{-1}$ . Full lines represent the best fits with Eq.(2) and power law behaviours at small and large  $C_w$  respectively. (b) Structural relaxation time behaviour with aging time  $t_w$  from Ref. (6) for colloidal suspensions of Laponite and (c) structural relaxation time behaviour with the inverse of temperature  $1/T$  from Ref. (17) for a metallic glass. (d)  $\beta$  parameter from Eq.(1) as a function of weight concentration for IPN microgel suspensions. Full line is a guide to eyes. (e)  $\beta$  exponent as a function of aging time  $t_w$  from Ref. (6, 53) for colloidal suspensions of Laponite and (f)  $\beta$  exponent dependence with  $1/T$  from Ref. (16) for a metallic glass.

IPN microgels represent therefore a good prototype to investigate the role of different parameters varied ad hoc in a single system. To broaden the investigated dynamical range for  $C_w > C_w^*$ , we focus our attention on particles with the highest PAAc content ( $C_{PAAc}=24.6\%$ ), as they allow to get closer to the critical weight concentration (see Fig.2(b)).

The corresponding structural relaxation time  $\tau$  is reported in Fig. 3(a). An interesting behaviour shows up: at low  $C_w$ ,  $\tau$  grows exponentially up to a critical weight concentration value  $C_w^*$  with a behaviour  $\tau = \tau_0 \exp(\frac{D_{C_w} C_w}{C_{w0} - C_w})$ . Above  $C_w^*$  it suddenly increases as a power law  $\tau \sim C_w^\alpha$  with  $\alpha = 2.6 \pm 0.1$  signing the existence of two different dynamical

regimes. A similar crossover has been recently reported for PNIPAM microgels (36) and share many similarities with the dynamics of hard colloids and structural glasses close to an out of equilibrium state. The relaxation time vs aging time  $t_w$  of an hard colloid, the largely studied Laponite<sup>®</sup> suspensions (4, 7, 54, 55), is reported in Fig. 3(b) from Ref. (6). It evolves from an exponential behaviour  $\tau = \tau_0 \exp(\frac{D t_w}{t_w^\infty - t_w})$  (3, 5, 6, 9) where  $t_w$  drives the system out of equilibrium and  $t_w^\infty$  sets the apparent divergence (56, 57), to a slower than Arrhenius dependence with increasing  $t_w$ . Fig. 3(c) shows instead the temperature dependence of the structural relaxation time for a metallic glass (17). Also in this case, widely investigated in the last years (16, 17, 58), the existence of two dynamical regimes below and above the glass transition temperature  $T_g$  has been observed. After  $T_g$  the weaker temperature dependence of the structural relaxation time is well described by an Arrhenius behaviour. It is worth to note that the dynamical crossover is reached by increasing concentration (Fig. 3(a)) or waiting time (Fig. 3(b)) in colloidal glasses and by decreasing temperature (Fig. 3(c)) in structural glasses. Our findings for IPN microgels suggest that a unifying scenario can be provided: the slowing down of the dynamics achieved by varying weight concentration (11, 36, 59), waiting time (3, 5, 6, 9) or temperature (16, 17) is accompanied by a super Arrhenius increase of the structural relaxation time followed by a slower than Arrhenius or an Arrhenius behaviour. Thus the existence of two different dynamical regimes is a general feature of soft colloids, hard colloids and structural glasses.

To complement these observations, we report in Fig. 3(d) the behaviour of the  $\beta$  parameter derived from the fits through Eq.(1). Surprisingly we find that the dynamical crossover at  $C_w^*$  is signaled by a sharp change of the shape parameter  $\beta$  from stretched ( $\beta < 1$ ) to compressed ( $\beta > 1$ ) in the high concentrated samples that we attribute to rising stresses deriving from the high packaging of the particles. As in the case of the

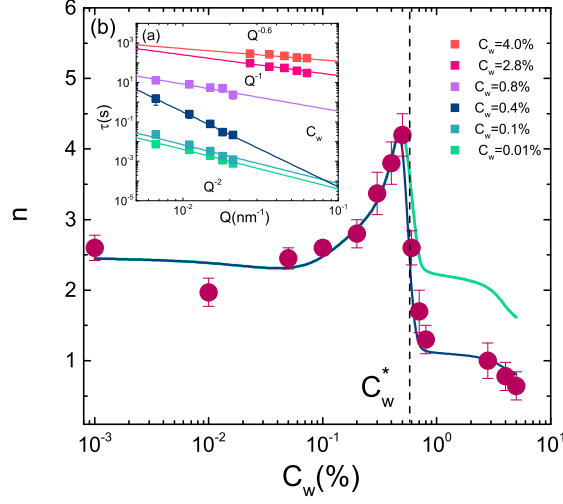


Figure 4: (a) Structural relaxation time as a function of the scattering vectors  $Q$  for IPN microgel suspensions at  $C_{PAAc}=24.6\%$  and  $T=311\text{ K}$  as measured through DLS and XPCS at increasing weight concentrations. Full lines represent the fits through Eq.5. (b) Power exponent from fits through Eq.5. Blue full line is the predicted behaviour from Eq.12 while green full line is the predicted behaviour using Eq.10.

structural relaxation time, the behaviour of  $\beta$  displays many similarities with that observed in the hard colloid of Ref. (6) as a function of  $t_w$  (Fig. 3(e)) and in the metallic glass of Ref. (17) as a function of  $1/T$  (Fig. 3(f)). For all these systems the dynamical crossover driven by  $C_w$ ,  $t_w$  or  $T$  is always accompanied by a discontinuity of  $\beta$ , as also found for PNIPAM microgels (36), corroborating the existence of a universal behaviour regardless of the control parameter and the specific interactions of the system. It is worth to note that in the first dynamical regime  $\beta$  decreases below 1 while in the second one it increases to values up to  $\simeq 1 \div 1.5$  depending on the system. This deviation from the common stretched behaviour can be attributed to the development of internal stresses at the transition (6, 11, 16, 25, 27). The peculiar values of each system depend on the specific material, on its history and/or on the preparation protocols whose optimization and control is subject of theoretical and experimental investigations.

The  $Q$ -dependence of the structural relaxation time in the range  $Q=(0.006 \div 0.063)$   $\text{nm}^{-1}$  is reported in Fig. 4(a) at different concentrations. The data are well fitted through a power law

$$\tau(Q) \propto Q^{-n} \quad (5)$$

shown as solid lines in Fig. 4(a). The behaviour of  $n$  as a function of weight concentration is reported in Fig. 4(b). Two dynamical regimes can be distinguished below and above  $C_w^*$ . In the first one ( $C_w < C_w^*$ )  $n$  increases from values typical of diffusive dynamics ( $n \sim 2$ ), to unusual values ( $n \sim 4$ ) for which diffusive dynamics is ruled out and an increase of viscosity is observed by eyes.

In the second dynamical regime ( $C_w \geq C_w^*$ )  $n$  suddenly decreases down to values  $n \leq 1$  where the case of  $n \sim 1$  is peculiar of the ballistic motion of particles. The crossover between the two dynamical regimes is characterized by a maximum in correspondence of the critical weight concentration  $C_w^*$  and is also associated to the observed crossover of the structural relaxation time (Fig. 3(a)) and  $\beta$  parameter (Fig. 3(d)). Aiming to explain this behaviour we consider that at low weight concentration  $C_w < 0.1$  % particles freely move, the diffusion process is well described by Fickian law, as in the case of Brownian motion, and the mean square displacement  $\langle r^2(t) \rangle$  has a linear time dependence:

$$\langle r^2(t) \rangle = 6Dt \quad (6)$$

where  $D$  is the particle diffusion coefficient. At increasing weight concentration  $C_w > 0.1$  % the system starts to become spatially heterogeneous, particles are no longer free to move as in the case of pure diffusive dynamics since they are trapped in cages characterized by different persisting times. In our experiments we probe scattering vectors  $Q$  in the range  $Q=(0.006 \div 0.063)$   $\text{nm}^{-1}$  that corresponds to length scales up to

ten particles radii ( $R = (130 \pm 2)$  nm) and we are thus sensitive to these heterogeneities. As a consequence Eq. 6 fails to reproduce the data which instead can be described by a non-Fickian anomalous diffusion (60):

$$\langle r^2(t) \rangle = \Gamma t^\beta \quad (7)$$

with an effective diffusion coefficient (61, 62)  $D(t) = \Gamma t^{\beta-1}$ . The *diffusive dynamics* (Eq. 6) is recovered when  $\beta = 1$  and  $D(t) = \Gamma = 6D$ . For  $0 < \beta < 1$  the dynamics is *subdiffusive* and for  $\beta > 1$  is *superdiffusive*, with the special case of  $\beta = 2$  corresponding to *ballistic* motion.

The mean square displacement, in the Gaussian approximation, is related to the intermediate scattering function as (47):

$$F(Q, t) = \exp(-Q^2 \langle r^2(t) \rangle / 6) \quad (8)$$

that, using the generalized mean square displacement of Eq. 7, becomes  $F(Q, t) = \exp(-\frac{Q^2 \Gamma}{6} t^\beta)$ . The comparison with the KWW expression (Eq.(1)) of the intermediate scattering function  $F(Q, t) \propto \exp(-(t/\tau(Q))^\beta)$ , gives  $(t/\tau(Q))^\beta = \frac{Q^2 \Gamma}{6} t^\beta$  and:

$$(1/\tau(Q))^\beta = Q^2 \Gamma / 6 \quad (9)$$

that provides:

$$\tau(Q) \propto Q^{-2/\beta} \quad (10)$$

In the case of diffusive dynamics with  $\beta = 1$  one gets the typical  $\tau(Q) \propto Q^{-2}$  behaviour while in the case of ballistic motion of particles with  $\beta = 2$   $\tau(Q) \propto Q^{-1}$ . A comparison between Eq.5 and Eq.10 gives  $n = 2/\beta$ . This behaviour is reported in Fig.4(b) as green

line. One can observe a good agreement with the experimental data only for  $C_w < C_w^*$ . The critical weight concentration  $C_w^*$ , characterized by a relaxation time of the order of seconds (Fig.3(a)), sets the transition from a fluid to an intermediate state that is visually arrested, as shown in the top photograph of Fig.3. For  $C_w \geq C_w^*$  the dynamics slows down progressively towards a glassy state, as witnessed by the increasing relaxation times up to values of the order of thousand seconds. Here the Gaussian approximation of Eq.8 becomes inaccurate (63) and a different scenario has to be invoked. The dynamics approaching the glassy state can be described within the Mode Coupling Theory (MCT) (64,65) that provides a different  $Q$ -dependence of the structural relaxation time:

$$\tau(Q) \propto Q^{-1/\beta} \quad (11)$$

Surprisingly for  $C_w \geq C_w^*$  a perfect agreement is now observed as shown in Fig.4(b) (blue full line). Therefore the experimental data are well described through:

$$\begin{aligned} \tau(Q) &\propto Q^{-2/\beta} & C_w < C_w^* \\ \tau(Q) &\propto Q^{-1/\beta} & C_w \geq C_w^* \end{aligned} \quad (12)$$

## 4 Conclusions

In conclusion through XPCS and DLS measurements we have shown that for IPN microgels interpenetrating different amount of PAAc into PNIPAM network originates particles with varying softness allowing to finely control the fragility of the system. Moreover, we find the existence of two dynamical regimes, with a crossover of the structural relaxation time associated to a clear change of the  $\beta$  exponent from stretched ( $\beta < 1$ ) to compressed ( $\beta > 1$ ). The comparison with similar behaviours found in hard colloids and in metallic glasses indicates that these are general common features of different sys-

tems regardless of the control parameters ( $C_w$ ,  $t_w$ , T) and of the specific interactions at stakes. The scattering vector dependence of the structural relaxation time in IPN microgels displays a surprising behaviour of the derived power exponent with a maximum in correspondence of the dynamical crossover. We provide an interpretation that well depict the experimental data: at very low concentration, when particles are free to move, the dynamics is well described by a Fickian diffusion, at intermediate concentrations, when particles start to be trapped in cages, an effective non Fickian anomalous diffusion has to be considered, while at the highest investigated concentrations, when the systems is going towards a glassy state, the emergence of a ballistic motion is well described within the Mode Coupling Theory. All these results contribute to the further understanding of the role of softness in the fragility, to the analogies and differences between colloidal and structural glasses and add new insights to the so far debated stretched to compressed transition. In order to further test our findings and hypothesis, more experiments on a wide range of systems will be useful.

**Acknowledgments:** The authors acknowledge acknowledge ESRF for beamtime and support from MIUR Fare SOFTART (R16XLE2X3L).

**Author Contributions** R.A., V.N. and B.Ruz. conceived the experiments. R.A., V.N., B.R., B.Ruz. and F.Z. conducted the experiments. R.A., V.N. and B.Ruz. analysed the results. M.B. and E.B. synthesized the samples. R.A., V.N. and B.Ruz. wrote the manuscript.

**Competing Interests** The authors declare that they have no competing financial interests.



## References

1. W. C. K. Poon, Phase separation, aggregation and gelation in colloid polymer mixtures and related systems. *Curr. Opin. Colloid Interface Sci.* **3**, 593-599 (1998).
2. E. Zaccarelli, Colloidal Gels: Equilibrium and Non-Equilibrium Routes. *J. Phys.: Condens. Matter* **19**, 323101-50 (2007).
3. M. Bellour, A. Knaebel, J. L. Harden, F. Lequeux, J. P. Munch, Aging processes and scale dependence in soft glassy colloidal suspensions. *Phys. Rev. E* **67**, 031405-8 (2003).
4. R. Bandyopadhyay, D. Liang, H. Yardimci, D. A. Sessoms, M. A. Borthwick, S. G. J. Mochrie, J. L. Harden, R. L. Leheny, Evolution of particle-scale dynamics in an aging clay suspension. *Phys. Rev. Lett.* **93**, 228302.
5. F. Schosseler, S. Kaloun, M. Skouri, J. P. Munch, Diagram of the aging dynamics in laponite suspensions at low ionic strength. *Phys. Rev. E* **73**, 021401.
6. R. Angelini, L. Zulian, A. Fluerasu, A. Madsen, G. Ruocco, B. Ruzicka, Dichotomic Aging Behavior in a Colloidal Glass. *Soft Matter* **9**, 10955-9 (2013).
7. R. Angelini, E. Zaccarelli, F. A. de Melo Marques, M. Sztucki, A. Fluerasu, G. Ruocco, B. Ruzicka, Glass-glass transition during aging of a colloidal clay. *Nat. Commun.* **5**, 4049-7 (2014).
8. P. Kwaśniewski, A. Fluerasu, A. Madsen, Anomalous dynamics at the hard-sphere glass transition. *Soft Matter* **10**, 8698-8704 (2014).

9. R. Angelini, B. Ruzicka, Non-diffusive dynamics in a colloidal glass: Aging versus rejuvenation. *Colloids and Surfaces A: Physicochemical and Engineering Aspects* **483**, 316-320 (2015).
10. R. Pastore, G. Pesce, M. Caggioni, Differential Variance Analysis: a direct method to quantify and visualize dynamic heterogeneities. *Scientific Reports* **7**, 43496-9 (2017).
11. L. Cipelletti, S. Manley, R. Ball, D. Weitz, Universal Aging Features in the Restructuring of Fractal Colloidal Gels. *Phys. Rev. Lett.* **84**, 2275-4 (2000).
12. H. Guo, S. Ramakrishnan, J. Harden, R. L. Leheny, Gel formation and aging in weakly attractive nanocolloid suspensions at intermediate concentrations. *J. Chem. Phys.* **135**, 154903-16 (2011).
13. L. Cristofolini, Synchrotron X-ray techniques for the investigation of structures and dynamics in interfacial systems. *Current Opinion in Colloid and Interface Science* **19**, 228-241 (2014).
14. C. Caronna, Y. Chushkin, A. Madsen, A. Cupane. *Phys. Rev. Lett.* **100**, 55702-4 (2008).
15. H. Conrad, F. Lehmkuhler, B. Fischer, F. Westermeier, M. A. Schroer, Y. Chushkin, C. Gutt, M. Sprung, G. Grübel, Correlated heterogeneous dynamics in glass-forming polymers. *Phys. Rev. E* **91**, 042309-6 (2015).
16. B. Ruta, Y. Chushkin, G. Monaco, L. Cipelletti, E. Pineda, P. Bruna, V. Giordano, M. Gonzalez-Silveira, Atomic-Scale Relaxation Dynamics and Aging in a Metallic Glass Probed by X-Ray Photon Correlation Spectroscopy. *Phys. Rev. Lett.* **109**, 165701-4 (2012).

17. Z. Evenson, B. Ruta, S. Hechler, M. Stolpe, E. Pineda, I. Gallino, R. Busch, X-Ray Photon Correlation Spectroscopy Reveals Intermittent Aging Dynamics in a Metallic Glass. *Phys. Rev. Lett.* **115**, 175701-4 (2015).
18. P. Falus, M. Borthwick, S. Narayanan, A. Sandy, S. Mochrie, Crossover from stretched to compressed exponential relaxations in a polymer-based sponge phase. *Phys. Rev. Lett.* **97**, 066102-4 (2006).
19. R. A. Narayanan, P. Thiagarajan, S. Lewis, A. Bansal, L. S. Schadler, L. B. Lurio, Dynamics and internal stress at the nanoscale related to unique thermomechanical behavior in polymer nanocomposites. *Phys. Rev. Lett.* **97**, 075505-4 (2006).
20. S. Srivastava and A.K. Kandar and J.K. Basu and M.K. Mukhopathyay and L.B. Lurio and S. Narayanan and .K. Sinha, Complex dynamics in polymer nanocomposites. *Phys. Rev. E* **79**, 021408-8 (2009).
21. V. Balitska, O. Shpotyuk, M. Brunner, I. Hadzaman, Stretched-to-compressed-exponential crossover observed in the electrical degradation kinetics of some spinel-metallic screen-printed structures. *Chemical Physics* **501**, 121-127 (2018).
22. J. P. Bouchaud, *Anomalous Relaxation in Complex Systems: From Stretched to Compressed Exponentials* (2008).
23. A. Nicolas, E. E. Ferrero, K. Martens, J.-L. Barrat, Disordered systems and neural networks deformation and flow of amorphous solids: An updated review of mesoscale elastoplastic models. *arXiv:1708.09194v2* (2018).
24. T. Morishita, Compressed exponential relaxation in liquid silicon: Universal feature of the crossover from ballistic to diffusive behavior in single-particle dynamics. *The Journal of Chemical Physics* **137**, 024510-6 (2012).

25. M. Bouzid and J. Colombo and L. V. Barbosa and E. Del Gado, Elastically driven intermittent microscopic dynamics in soft solids. *Nat. Comm.* **8**, 15846-8 (2017).
26. R. Pastore and G. Pesce and A. Sasso and M. Pica Ciamarra , Many facets of intermittent dynamics in colloidal and molecular glasses. *Colloids and Surfaces A: Physicochemical and Engineering Aspects* **532**, 87-96 (2017).
27. Z. W. Wu, W. Kob, W. Wang, L. Xu, Stretched and compressed exponentials in the relaxation dynamics of a metallic glass-forming melt. *Nature Communication* **9** (2018).
28. P. E. Ramírez-González, M. Medina-Noyola, Glass transition in soft-sphere dispersions. *Journal of Physics: Condensed Matter* **21**, 075101-13 (2009).
29. D. Vlassopoulos, M. Cloitre, Tunable rheology of dense soft deformable colloids. *Current Opinion in Colloid & Interface Science* **19**, 561-574 (2014).
30. R. H. Pelton, Temperature-sensitive aqueous microgels. *Adv. Colloid Interface Sci.* **85**, 1–33 (2000).
31. T. Hellweg, C. Dewhurst, E. Brückner, K.Kratz, W.Eimer, Colloidal crystals made of poly(N-isopropylacrylamide) microgel particles. *Colloid. Polym. Sci.* **278**, 972-978 (2000).
32. L. A. Lyon, A. Fernandez-Nieves, The Polymer/Colloid Duality of Microgel Suspensions. *Annu. Rev. Phys. Chem.* **63**, 25-43 (2012).
33. R. P. Seekell, P. S. Sarangapani, Z. Zhangb, Y. Zhu, Relationship between particle elasticity, glass fragility, and structural relaxation in dense microgel suspensions. *Soft Matter* **11**, 5485-5491 (2015).

34. S. K. Behera, D. Saha, P. Gadige, R. Bandyopadhyay, Effects of polydispersity on the glass transition dynamics of aqueous suspensions of soft spherical colloidal particles. *Physical Review Materials* **1**, 055603 (2017).
35. N.Gnan, L. Rovigatti, M. Bergman, E. Zaccarelli, In Silico Synthesis of Microgel Particles. *Macromolecules* **50**, 8777 (2017).
36. A.-M. Philippe, D. Truzzolillo, J. Galvan-Myoshi, P. Dieudonné-George, V. Trappe, L. Berthier, L. Cipelletti, Glass transition of soft colloids. *Phys. Rev. E* **97**, 040601 (2018).
37. X. Xia, Z. Hu, Synthesis and Light Scattering Study of Microgels with Interpenetrating Polymer Networks. *Langmuir* **20**, 2094–2098 (2004).
38. J. Mattsson, H. M. Wyss, A. Fernandez-Nieves, K. Miyazaki, Z. Hu, D. Reichman, D. A. Weitz, Soft colloids make strong glasses. *Nature* **462**, 83–86 (2009).
39. J. Ma, B. Fan, B. Liang, J. Xu, Synthesis and characterization of Poly(N-isopropylacrylamide)/Poly(acrylic acid) semi-IPN nanocomposite microgels. *J. Colloid Interface Sci.* **341**, 88–93 (2010).
40. X. Liu, H. Guo, L. Zha, Study of pH/temperature dual stimuli-responsive nanogels with interpenetrating polymer network structure. *Polymers* **61**, 1144–1150 (2012).
41. V. Nigro, R. Angelini, M. Bertoldo, V. Castelvetro, G. Ruocco, B. Ruzicka, Dynamic light scattering study of temperature and pH sensitive colloidal microgels. *J. Non-Cryst. Solids* **407**, 361-366 (2015).

42. V. Nigro, R. Angelini, M. Bertoldo, F. Bruni, M. Ricci, B. Ruzicka, Dynamical behavior of microgels of interpenetrated polymer networks. *Soft Matter* **13**, 5185-5193 (2017).
43. A. Madsen, R. Leheny, H. Guo, M. Sprung, O. Czakkel, Beyond simple exponential correlation functions and equilibrium dynamics in X-ray photon correlation spectroscopy. *New J. of Phys.* **12**, 055001-16 (2010).
44. V. Nigro, R. Angelini, M. Bertoldo, F. Bruni, M. Ricci, B. Ruzicka, Local structure of temperature and pH-sensitive colloidal microgels. *J. Chem. Phys.* **143**, 114904-9 (2015).
45. V. Nigro, R. Angelini, M. Bertoldo, B. Ruzicka, Swelling of responsive-microgels: experiments versus models. *Colloids Surf. A* **532**, 389-396 (2017).
46. V. Nigro, R. Angelini, B. Rosi, M. Bertoldo, E. Buratti, S. Casciardi, S. Sennato, B. Ruzicka, Study of network composition in interpenetrating polymer networks of poly(n isopropylacrylamide) microgels: The role of poly(acrylic acid). *Journal of Colloid and Interface Science* **545**, 210 - 219 (2019).
47. J. P. Hansen, I. McDonald, *Theory of Simple Liquids with Applications to Soft Matter* (Academic Press, 2013).
48. C. Angell, The old problems of glass and the glass transition, and the many new twists. *Proc. Natl. Acad. Sci. USA* **92**, 6675-6682 (1995).
49. P. V. der Scheer, T. van de Laar, J. van der Gucht, D. Vlassopoulos, J. Sprakel, Fragility and Strength in Nanoparticle Glasses. *ACS Nano* **11**, 6755-6763 (2017).

50. N. Gnan, E. Zaccarelli, The microscopic role of deformation in the dynamics of soft colloids. *Nature Physics* (2019).
51. S. Sengupta, F. Vasconcelos, F. Affouard, S. Sastry, Dependence of the fragility of a glass former on the softness of interparticle interactions. *J. Chem. Phys.* **135**, 194503-9 (2011).
52. Z. Shi, P. G. Debenedetti, F. H. Stillinger, P. Ginart, Structure, dynamics, and thermodynamics of a family of potentials with tunable softness. *J. Chem. Phys.* **135**, 084153-9 (2011).
53. V. Tudisca, M. Ricci, R. Angelini, B. Ruzicka, Isotopic effect on the aging dynamics of a charged colloidal system. *RSC Advances* **2**, 11111-11116 (2012).
54. H. Tanaka, S. Jabbari-Farouji, J. Meunier, D. Bonn, Kinetics of ergodic-to-nonergodic transitions in charged colloidal suspensions: Aging and gelation. *Phys. Rev. E* **71**, 021402-9 (2005).
55. B. Ruzicka, E. Zaccarelli, L. Zulian, R. Angelini, M. Sztucki, A. Moussaïd, T. Narayanan, F. Sciortino, Observation of empty liquids and equilibrium gels in a colloidal clay. *Nat. Mater.* **10**, 56-60 (2011).
56. B. Ruzicka, L. Zulian, G. Ruocco, Routes to gelation in a clay suspension. *Phys. Rev. Lett.* **93**, 258301-4 (2004).
57. D. Saha, J. M. Yogesh, R. Bandyopadhyay, Investigation of the dynamical slowing down process in soft glassy colloidal suspensions: comparisons with supercooled liquids. *Soft Matter* **10**, 3292-3300 (2014).

58. B. Ruta, E. Pineda, Z. Evenson, Relaxation processes and physical aging in metallic glasses. *J. Phys.: Condens. Matt.* **29** (2017).
59. Q. Li, X. Peng, G. B. McKenna, Long-term aging behaviors in a model soft colloidal system . *Soft Matter* **13**, 1396-1404 (2017).
60. S. Havlin, D. Ben-Avraham, Diffusion in disordered media. *Advances in Physics* **36**, 695-798 (1987).
61. I. M. Sokolov, Models of anomalous diffusion in crowded environments. *Soft Matter* **8**, 9043-9052 (2012).
62. M. Palombo, A. Gabrielli, V. D. P. Servedio, G. Ruocco, S. Capuani, Structural disorder and anomalous diffusion in random packing of spheres. *Sci. Rep.* **3**, 2631-7 (2013).
63. U. Balucani, M. Zoppi, *Dynamics of the Liquid State*, vol. 10 of *Oxford Series on Neutron Scattering in Condensed Matter (Book 10)* (Clarendon Press; 1 edition, 1995).
64. C. Bennemann, J. Baschnagela, W. Paul, Molecular-dynamics simulation of a glassy polymer melt: Incoherent scattering function. *Eur. Phys. J. B* **10**, 323–334 (1999).
65. W. Götze, *Götze Complex Dynamics of Glass-Forming Liquids-A Mode-Coupling Theory*, International Series of Monographs on Physics (Oxford University Press, USA, 2009).